ADVANCED MATERIALS INTERFACES

www.advmatinterfaces.de

Switching the Electronic Properties of ZnO Surfaces with Negative T-Type Photochromic Pyridyl-dihydropyrene Layers and Impact of Fermi Level Pinning

Qiankun Wang, Giovanni Ligorio, Raphael Schlesinger, Valentin Diez-Cabanes, David Cornil, Yves Garmshausen, Stefan Hecht, Jérôme Cornil,* Emil J. W. List-Kratochvil,* and Norbert Koch**

Remote control of the electronic energy levels by external stimuli such as light will enable optoelectronic devices with improved or additional functionalities. Here, it is demonstrated that the electronic properties of ZnO interfaced with negative T-type photoswitches, that is, pyridyl-dihydropyrene (Py-DHP), can indeed be photomodulated. The process of forward switching of Py-DHP with green light from an isomer with a low energy gap to an isomer with a wider one is followed by a thermally activated backward transfer. Using photoemission spectroscopy and density functional theory modeling, it is shown that Py-DHP ring closure/opening reactions result in a reversible shift of frontier occupied molecular levels by 0.7 eV with respect to the Fermi level. Notably, in both molecular configurations, the energy level alignment at ZnO/Py-DHP interfaces is governed by a Fermi level pinning at the lowest unoccupied molecular level. Moreover, upon switching, an increase in the ionization energy for Py-DHP multilayers compared to that of a monolayer is observed. This is attributed to a different preferred molecular orientation in monolayer versus multilayers. The results show that a dynamic tuning of the energy level alignment at inorganic/organic interfaces by external stimuli is feasible and will aid the development of photoprogrammable optoelectronic devices.

1. Introduction

Hybrid organic/inorganic semiconductor interfaces have attracted attention due to their potentially superior charge transfer and injection efficiency for (opto)electronic applications,[1–5] such as light-emitting/sensing structures[6,7] and organic field-effect transistors (OFET).[2] Substantial efforts have been devoted to engineering the interfaces with regard to their energy level alignment in order to tune interfacial energy barriers, hence tailoring the charge carrier injection as well as extraction, and enhancing and expanding the functionality of electronic and optoelectronic devices.[6,8–10] For example, the use of interfacial layers (as thin as monolayers) composed of strong electron acceptor and donor molecules has proven feasible to substantially tune hole and electron injection/extraction properties, respectively.[6,9] However, this approach is limited to a static modification of the energy levels at the interface. More recently, the use of molecular switches has been shown to enable a *dynamic* energy level tuning,[11–13] which gives the interface multifunctional properties since the energy level alignment can be controlled and programmed via external stimuli, even in fully processed and encapsulated device stacks. These molecular compounds can be reversibly switched between two isomers by external stimuli, such as light, heat, and pH changes.[14,15] The switching between the two isomers fundamentally changes the electronic properties of the molecular compound, for example, the energy gap, the ionization

Q. Wang, Dr. R. Schlesinger, Prof. N. Koch
Institut für Physik and IRIS Adlershof
Humboldt-Universität zu Berlin
Brook-Taylor-Str. 6, 12489 Berlin, Germany
E-mail: norbert.koch@physik.hu-berlin.de

Dr. G. Ligorio, Prof. E. J. W. List-Kratochvil
Institut für Physik
Institut für Chemie and IRIS Adlershof
Humboldt-Universität zu Berlin
Brook-Taylor-Str. 6, 12489 Berlin, Germany
E-mail: emil.list-kratochvil@hu-berlin.de

The ORCID identification number(s) for the author(s) of this article can be found under https://doi.org/10.1002/admi.201900211.

V. Diez-Cabanes, Dr. D. Cornil, Prof. J. Cornil
Laboratory for Chemistry of Novel Materials
University of Mons
Place du Parc 20, B-7000 Mons, Belgium
E-mail: jerome.cornil@umons.ac.be

Y. Garmshausen, Prof. S. Hecht
Department of Chemistry and IRIS Adlershof
Humboldt-Universität zu Berlin
Brook-Taylor-Str. 2, 12489 Berlin, Germany
E-mail: sh@chemie.hu-berlin.de

Prof. N. Koch
Helmholtz-Zentrum Berlin für Materialien und Energie GmbH
Albert-Einstein Str. 15, 12489 Berlin, Germany

DOI: 10.1002/admi.201900211

energy and electron affinity, the molecular dipole moment,[11] as well as carrier mobility in blends with other organic semiconductors.[16,17] Thus, once the molecular switch is combined with other materials, the isomerization results in dynamically controlled heterointerfaces as well as bulk semiconductor properties.

So far, mostly diarylethenes,[15] azobenzenes,[18] and spiropyrans,[14] have been studied as photochromic components in hybrid structures. However, the switching of these molecules is either triggered with ultraviolet (UV) light illumination or accompanied by significant geometrical changes, which is problematic in solid-state devices due to UV-induced photodegradation or steric hindrance, respectively. Dihydropyrenes (DHPs) constitute another class of photochromic molecules. DHPs show promising potential for device applications, since upon switching—contrary to other photochromic systems—they do not undergo large geometrical changes, but rather changes in conjugation due to ring closure/opening. DHP derivatives exhibit negative T-type photochromism, implying that the switching process is thermally reversible. When irradiated with light with a photon energy larger than the optical energy gap (typically exceeding 2.0 eV) in the forward switching process, the π-conjugation of the molecule is interrupted and the energy gap increases. This leads to the open form of the DHP molecule. The process of forward switching with light is followed by a thermally activated backward reaction.[19] Another practically relevant aspect of DHPs is that the molecular core can be modified with a wide range of substituents that allow tuning of the energy gap and other electronic and switching properties for optimized integration in photoswitchable devices.[20,21]

Here, we report on pyridyl-DHP (Py-DHP; see the Supporting Information for synthesis), which can be switched reversibly upon visible light illumination and has a thermally activated back reaction at moderate temperature, in conjunction with the inorganic semiconductor ZnO. The pyridine moiety of Py-DHP (see **Figure 1**a) is expected to function as an anchoring group to the inorganic surfaces, assisting in forming ordered molecular structures. We demonstrate that the Py-DHP interlayers are able to reversibly modify the electronic properties of ZnO surfaces, here polar Zn-terminated ZnO(0001) and O-terminated ZnO(000-1). ZnO has been mostly used as an electron transport layer (when highly doped) in hybrid optoelectronic devices due to its high electron mobility, wide bandgap, and easy processability at low temperature.[6] The ability to modify its surface electronic properties in a dynamic manner would lead to a reversible control of interfacial charge injection/extraction properties, thus enabling multifunctional ZnO-based devices. The Py-DHP switching induced changes in the valence electronic structure and the core levels are investigated by ultraviolet photoelectron spectroscopy (UPS) and X-ray photoelectron spectroscopy (XPS). Theoretical calculations at the density functional theory (DFT) level are performed to assist the interpretation of the experimental observations. Py-DHP is switched in situ between its closed and open form, either by illumination with green light (λ = 565 nm) or mild heat treatment (at 50 °C). The position of the highest occupied molecular orbital (HOMO) level

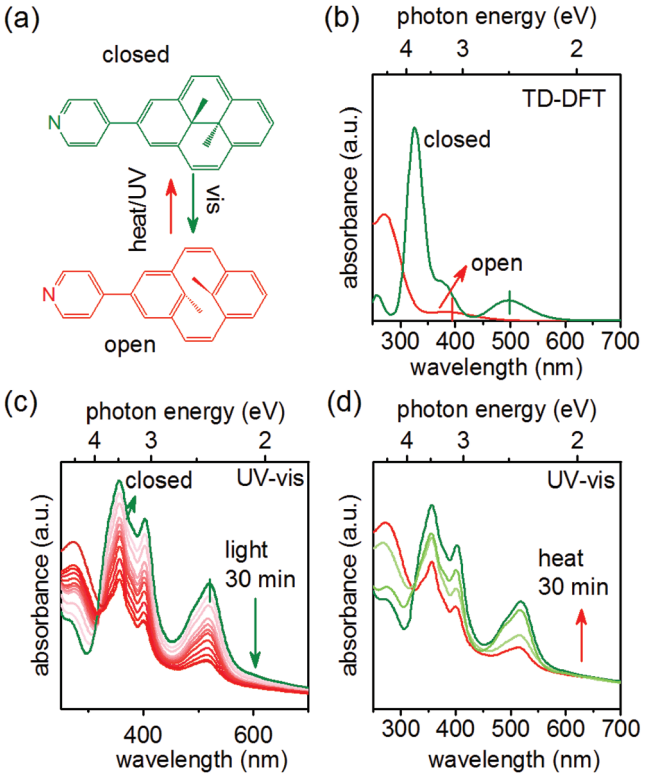

Figure 1. Ring opening/closure of the Py-DHP switch. a) Switching between the two isomers can be triggered by visible light (ring opening) and heat or UV light (ring closure). c,d) The ring opening process of the Py-DHP film (10 nm) reaches a photothermal equilibrium after ≈30 min illumination (λ = 565 nm, I_{max} > 200 mW cm^{-2}) and can be reset by heat treatment (50 °C), as displayed by UV–vis absorption spectra. b) Calculated absorption spectra of Py-DHP by time-dependent DFT (TD-DFT) are also plotted for sake of a comparison.

of Py-DHP exhibits a reversible massive shift of 0.7 eV with respect to the Fermi level (E_F) between the closed and open form. We find a higher ionization energy (IE) for Py-DHP in the multilayer regime compared to the monolayer, for both closed and open form. We attribute this to a transition of the average molecular orientation from preferentially standing up in the monolayer regime to a lying down or at least more inclined fashion in multilayers. Our findings provide thus a solid basis for incorporation of Py-DHP switches in ZnO-based multifunctional devices.

2. Results and Discussion

2.1. Switching Properties of Py-DHP

We first discuss switching of a 10 nm thick Py-DHP film on a quartz substrate by UV–vis spectroscopy. Figure 1c displays the spectral evolution of Py-DHP upon green light illumination to induce the ring opening reaction and subsequent heat treatment (Figure 1d) for the reverse reaction. The spectrum of Py-DHP in its original closed form (green line) exhibits an absorption maximum at ≈530 nm. Upon green light illumination, the absorption of closed Py-DHP attenuates gradually, accompanied by an

enhancement of the absorption in the UV region (≈300 nm). These changes occur due to the aforementioned ring opening reaction. After 30 min of illumination, no further changes in the spectra are observed, indicating that the photoswitching of initially closed Py-DHP reaches a photothermal equilibrium. The film was then in situ heated at 50 °C (see Figure 1d) to switch Py-DHP back to its closed form. Within 30 min of heat treatment, the spectral appearance is restored to that observed initially for closed Py-DHP, evidencing a high switching efficiency of Py-DHP back to its closed form. We performed time-dependent DFT (TD-DFT) calculations (Figure 1b) to substantiate the spectral assignments from the experiments. From the calculations, we find that the lowest absorption peak lies at 510 nm for closed Py-DHP (green dashed line), in agreement with the experimental data. For open Py-DHP, the lowest energy absorption peak is predicted at 400 nm (red dashed line). Notably, in experiment, the absorption peak at ≈530 nm does not disappear completely upon green light illumination. We attribute such incomplete photoswitching of the closed Py-DHP primarily to thermal back-switching of the open form occurring already at room temperature at a moderate rate.[22] The switching efficiency of closed to open Py-DHP is estimated to be ≈80% at room temperature by comparing the absorption intensity in the visible region after subtracting the Rayleigh scattering background.

2.2. Electronic Properties of ZnO/Py-DHP Interfaces from Photoelectron Spectroscopy

UPS and XPS measurements were performed in order to access how the electronic properties of Py-DHP and the interface with ZnO change upon switching. **Figure 2** displays UPS spectra of Py-DHP for the mono- and multilayer regime (nominal mass thickness of 10 and 100 Å, respectively) on both ZnO polar faces upon switching back and forth (by green light illumination and heating). For bare ZnO(0001) (top left inset in Figure 2a), the valence band maximum (VBM) and the work function (ϕ) are measured at 3.3 and 3.7 eV, respectively. This is in line with previously reported values for clean ZnO(0001).[9] For the 10 Å Py-DHP film (originally in its closed form) on ZnO, that is, approximately monolayer coverage, no ϕ change was observed upon molecular film deposition, and the low binding energy onset of the HOMO level of closed Py-DHP is found 1.8 eV below E_F, with the peak at ≈2.8 eV, as determined by the fitting of Py-DHP spectra (see Figure S1 and Table S1, Supporting Information). The sample was subsequently illuminated with green light for 30 min. As a result, Py-DHP switched from the closed to the open form, and accordingly the spectral features in the valence region change. Most prominently, the clear HOMO-derived feature of closed Py-DHP (centered at 2.8 eV binding energy) becomes strongly attenuated.

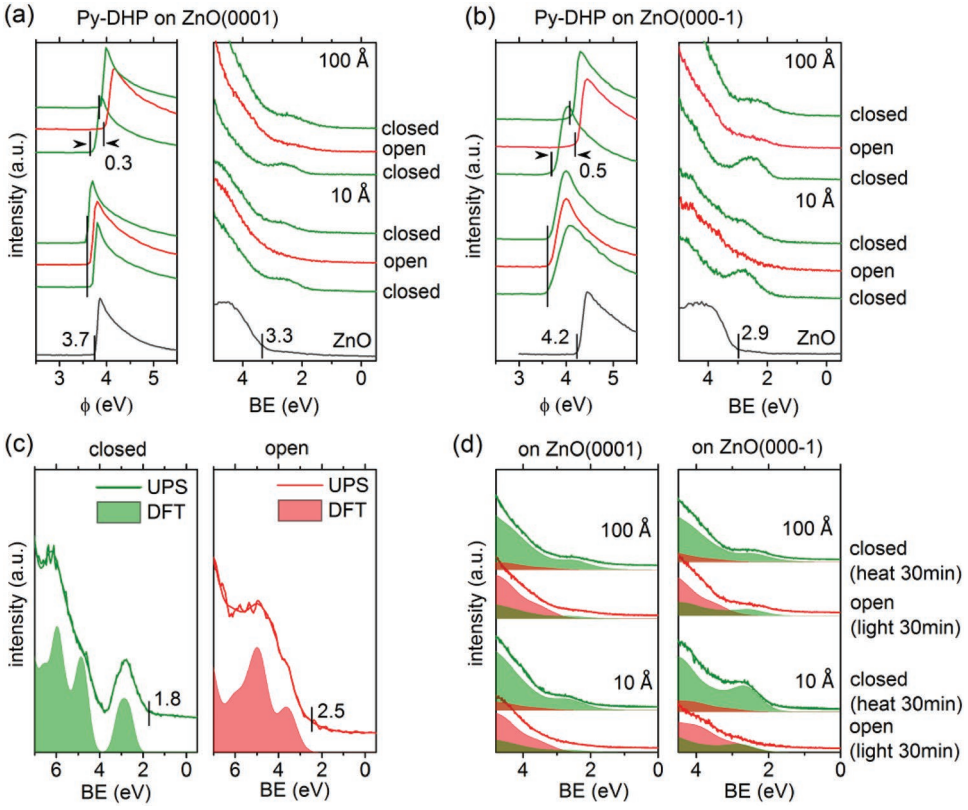

Figure 2. a,b) UPS spectra of 10 and 100 Å Py-DHP films evaporated on ZnO(0001) and ZnO(000-1) surfaces. For each film, in situ switching was realized through the illumination by green light (565 nm), which switches the molecule from the closed to the open form (red line), and through heating at 50 °C for switching back to its closed form (green line). c) UPS spectra (substrate signal subtracted) and DFT calculated density of states (DOS) of the closed and open Py-DHP molecules. The DFT calculated spectra were shifted by 0.4 eV for aligning the experimental results. In the calculations, photoemission cross sections have not been taken into account. d) Decomposition of the sample spectra into closed and open Py-DHP contributions.

Despite our estimation above that the switching efficiency is ≈80% (corresponding to equilibrium at room temperature), the valence electronic features of open Py-DHP film can be hardly discerned in the UPS spectra. This is because the signal from residual closed Py-DHP is still present as well as (small) contributions from the ZnO substrate in the energy range above 3 eV. To better display the signal for the open form, Figure 2c shows the UPS data for which the signal of ZnO as well as that of the closed Py-DHP was appropriately scaled and subtracted. With this procedure, the valence features of open Py-DHP are well observable, and we identify the HOMO level onset at 2.5 eV binding energy (peak center at 3.5 eV, see Figure S1, Supporting Information). Thus, the ring opening induced gap renormalization places the HOMO level onset 0.7 eV farther away from E_F, in line with qualitatively similar observations made for other photoswitches.[11] Next, the sample was heated in situ to a temperature of 50 °C for 30 min in order to induce the reverse ring-closure reaction. The reappearance of the closed Py-DHP HOMO with its onset at 1.8 eV binding energy is observed, confirming that Py-DHP molecules are indeed switched back to their closed form. To corroborate these findings of the different electronic properties—most notably the HOMO feature—of open and closed Py-DHP molecules, we modeled the electronic structure at the DFT level using the PBE functional. The UPS spectra of both open and closed Py-DHP films can be well reproduced by the calculated density of states (DOS) of the molecules (shown in Figure 2c), confirming that the valence electronic features of the open and closed Py-DHP are vastly different. With the subtracted UPS spectra of open and closed Py-DHP, the experimental UPS spectra of the monolayer film after switching by green light can be quantitatively fitted with two contributions (see Figure 2d). Hereby, we obtain a fraction of ≈80% open Py-DHP and 20% closed Py-DHP. This ratio is consistent with the switching efficiency observed in the UV–vis measurements. Applying the same procedure to the spectra after the heat-induced back-switching into the closed state, we obtain 95% closed Py-DHP and 5% open Py-DHP, thus a very high yield of back-switching.

To study how switching of Py-DHP in thicker films impacts the interface electronic properties, we first increased the organic layer thickness to nominally 50 Å (see Figure S2, Supporting Information), and subsequently to 100 Å on both ZnO surfaces. We observe that the HOMO onset of the closed Py-DHP thick films is still at 1.8 eV, where it was also found for the monolayer. Upon inducing switching by green light illumination and subsequent heat treatment, we observe that in the multilayer regime Py-DHP also exhibits a reversible switching behavior. Equivalent to our results for the monolayer, the ring opening reaction is accompanied by the disappearance of the closed Py-DHP HOMO feature (onset at 1.8 eV binding energy and peak at 2.8 eV) and the corresponding reappearance of the open Py-DHP (onset at 2.5 eV binding energy and peak at ≈3.5 eV) (again deduced from difference spectra). Subsequent heat treatment expectedly restores the HOMO feature of closed Py-DHP in the valence region (Figure 2a).

However, in contrast to the monolayer coverage regime, where ϕ stayed constant upon switching, in the multilayer regime the switching (ring opening) leads to a ϕ increase by 0.2 eV/0.3 eV for 50 Å/100 Å thick Py-DHP films, respectively. Moreover, this switching-induced change of ϕ was not fully reversible, as seen from the sequence of SECO spectra in Figure 2a,b.

To obtain a wider insight into Py-DHP/ZnO interface properties, we also investigated Py-DHP deposited on oxygen terminated ZnO(000-1) (see Figure 2b). This surface, in its pristine state, exhibits the VBM at 2.9 eV and a ϕ of 4.2 eV. Deposition of a 10 Å thick Py-DHP film (equivalent to approximately a monolayer) results in a decrease of the work function from 4.2 to 3.6 eV. In contrast, for Py-DHP on ZnO(0001) we observed no change in ϕ. Yet, the ϕ values for (closed) Py-DHP monolayer coverage on both ZnO surfaces are virtually identical. Accordingly, we observe the HOMO onset of Py-DHP on ZnO(000-1) also at 1.8 eV binding energy. Reversible switching of Py-DHP on ZnO(000-1) could be induced by green light illumination and heat treatment, as shown in Figure 2b. According to the decomposition of the spectra (Figure 2d), the HOMO onset for open Py-DHP is at 2.5 eV as well. The work function of monolayer Py-DHP also stays constant during switching. In contrast, also on ZnO(000-1), one observes an increase in the multilayer ϕ upon switching the molecules. Quantitatively, the switching-induced ϕ change is similar, yet a little larger than on ZnO(0001). For the 50 Å (see Figure S2, Supporting Information) and 100 Å thick films, we observe ϕ increases by 0.3 and 0.5 eV after switching, respectively. On ZnO(0001), the corresponding values were 0.2 and 0.3 eV.

The energy level alignment for Py-DHP on both ZnO faces, for mono- and multilayer coverage, as well as changes upon switching, as discussed above, are summarized in **Figure 3**. Clearly, one recognizes that a simple energy level alignment model, such as the Schottky–Mott limit with a constant

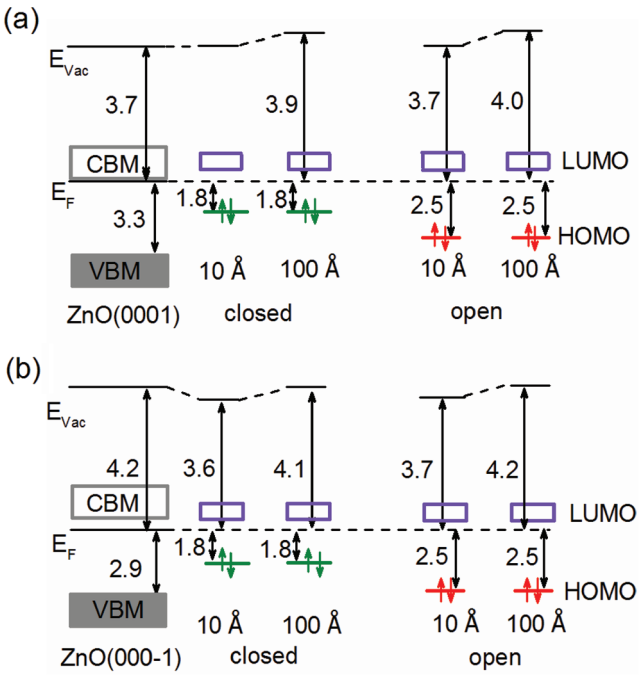

Figure 3. a,b) Schematic energy level diagram of Py-DHP/ZnO(0001) and Py-DHP/ZnO(000-1) interfaces. All values are in the unit of eV. Energy positions of vacuum level (E_{vac}), VBM, HOMO with respect to the Fermi level (E_F) are derived from UPS measurements.

electrostatic potential across the interfaces, cannot explain all data at hand. As a starting point to elucidate the rather complex situation, we consider that Py-DHP has an intrinsic dipole moment, primarily along the long molecular axis. This is easily rationalized from the fact that the pyridine group is polar and that the Py-DHP monolayer with this "anchoring group" will preferentially align upright on the surfaces, as discussed by Hofmann et al.[23] With this, one could qualitatively explain the work function reduction by 0.6 eV found for ZnO(000-1). However, this then raises the question why on both ZnO surfaces the same monolayer ϕ values are observed, that is, why does ϕ stay constant when depositing Py-DHP onto ZnO(0001). Consequently, there must be (at least) one more process involved, lowering the electrostatic potential at the interface with ZnO(000-1). Such a process could be Fermi level pinning. However, adding the optical gap as deduced from UV–vis results (2.1 eV for the closed and 2.9 eV for the open form, respectively) to the measured HOMO position, as well as adding a lower limit value for the exciton binding energy of 0.3–0.4 eV,[24] we estimate that the molecular LUMO level onset is still ≈0.5 eV above E_F in all experiments (see Figure 3). While pinning at 0.5 eV below the LUMO is not unprecedented in literature[25,26] (particularly since gap states of low density may be sufficient for pinning), our speculation is not unequivocal. Therefore, we performed calculations at the DFT level to further understand the electronic properties at the ZnO/Py-DHP interface, as discussed in the following section.

2.3. DFT Calculations of ZnO/Py-DHP Interfaces and Comparison with Experimental Data

We first compute the dipole moment of the isolated closed and open Py-DHP isomers in the gas phase, and find it to be 3.4 and 3.5 D, respectively (direction from pyridine as negative pole to DHP as positive pole, see Figure S3 and Table S2, Supporting Information), along the molecular backbone. These values are large enough to allow ϕ reductions of the experimentally observed magnitude. The very similar magnitude of the dipoles in the two states explains the absence of ϕ changes upon switching in the monolayer. However, for improved understanding of the actual interfaces between Py-DHP and ZnO and to explicitly account for depolarization effects affecting individual dipoles, we grafted the open and closed Py-DHP isomer onto both polar ZnO surfaces. To do so, we estimate experimentally the density of Py-DHP in the monolayer from the C1s core level region and the attenuation of the underlying ZnO related core levels (see Figure S5, Supporting Information, for details) and select the size of the unit cell for the calculations based on this value.

The adsorption energies of Py-DHP on ZnO are computed in order to evaluate the stability of Py-DHP on ZnO. As displayed in Table S3 (Supporting Information), they are calculated as the difference between the energy of the adsorbed system and the sum of the energies of the free isolated molecules and bare passivated ZnO. Py-DHP on ZnO(000-1) is more stable by 0.5 eV per molecule than on ZnO(0001). Similar to the behavior of other pyridine moieties on polar ZnO,[27] Py-DHP is stabilized on ZnO(000-1) by a hydrogen bond between the pyridine and adjacent hydrogen atoms. On the contrary, on ZnO(0001) the interactions between the pyridine and surface Zn atoms are reduced due to the presence of hydroxyl groups. Nevertheless, on both faces, Py-DHP assumes a mostly upright conformation with the pyridine group facing the substrate (see Figure S4, Supporting Information, for structures).

As described in previous studies,[27,28] we investigated next the details of the change of the work function ($\Delta\phi$) by decomposing it into the following partition

$$\Delta\phi = \mathrm{BD} + \Delta V_{\text{Py-DHP}} + \Delta\phi_{\text{ZnO}} \quad (1)$$

where BD is the bond dipole at the ZnO/Py-DHP interface due to charge reorganization at the interface, $\Delta V_{\text{Py-DHP}}$ is the potential shift due to the intrinsic dipole moment of the Py-DHP monolayer, and $\Delta\phi_{\text{ZnO}}$ is the work function change in the ZnO slab alone caused by deformations due to Py-DHP adsorption. The BD, in conjunction with the charge density difference ($\Delta\rho$), of the system is plotted in **Figure 4**. $\Delta\rho$ is defined as

$$\Delta\rho = \rho_{\text{ZnO/Py-DHP}} - \rho_{\text{ZnO}} - \rho_{\text{Py-DHP}} \quad (2)$$

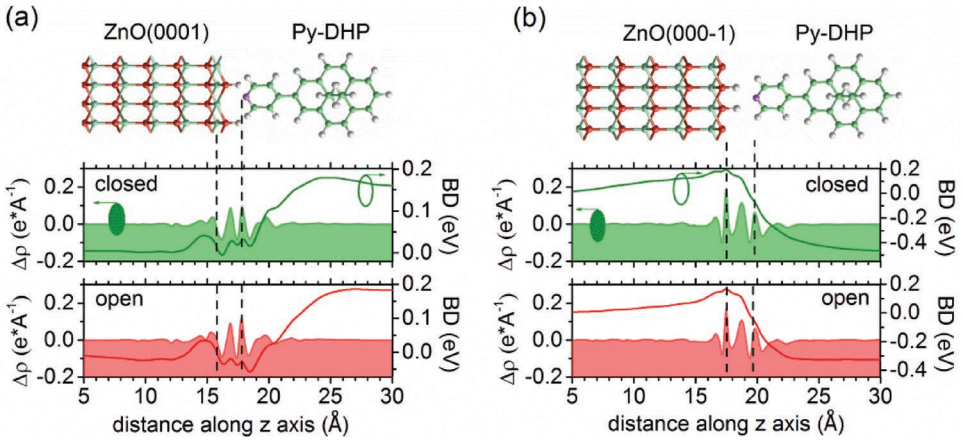

Figure 4. a,b) Plane averaged charge density difference ($\Delta\rho$) and corresponding bond dipole (BD) potential for Py-DHP on ZnO(0001) and Py-DHP on ZnO(000-1), respectively. The positions of the topmost Zn or O layer in ZnO and the N layer in Py-DHP are indicated by the vertical dashed lines.

with $\rho_{ZnO/Py\text{-}DHP}$ the charge density of the full ZnO/Py-DHP interface in its final geometry, ρ_{ZnO} that of the ZnO surface, and $\rho_{Py\text{-}DHP}$ the charge density of the Py-DHP monolayer, both in the interface geometry. It is seen that $\Delta\rho$ exhibits similar distributions along the surface normal for both closed and open forms. A Bader charge population analysis (in Table S3, Supporting Information) reveals that a minute amount of 0.02 |e| is transferred from Py-DHP to ZnO(0001), whereas on ZnO(000-1) the direction of charge transfer is reversed and slightly larger with 0.04 |e|. Consequently, the direction of the bond dipole is reversed for the two different ZnO surfaces. However, the magnitude of this charge transfer is very small and the BD contributions vary typically between 0.2 and 0.4 eV in absolute magnitude (Figure 4). Next, we turn to the other components of $\Delta\phi$. For $\Delta V_{Py\text{-}DHP}$, we consider an isolated monolayer of Py-DHP molecules with the same geometry as that when adsorbed on ZnO. We then compute the plane-averaged electrostatic potential across this organic layer. For $\Delta\phi_{ZnO}$, we rely on the equation $\Delta\phi_{ZnO} = \phi_{ZnO} - \phi_0$, where ϕ_{ZnO} is the work function of the ZnO surface after removing Py-DHP and ϕ_0 is the work function of the pristine ZnO surface. $\Delta\phi$ and its three components are summarized in **Table 1**. For both ZnO surfaces, not only the BD contribution is small but also $\Delta\phi_{ZnO}$; almost all of the ϕ reduction actually stems from the molecular contribution ($\Delta V_{Py\text{-}DHP}$ in Equation (1)) with only minor differences between the open and the closed isomer. This confirms the experimental findings that switching of the Py-DHP monolayer does not result in notable ϕ changes. However, there exists a sizeable difference between the calculated and measured $\Delta\phi$, since the calculations provide values of −1.2 and −1.6 eV for ZnO(0001) and ZnO (000-1), respectively, whereas experiments yield 0 and −0.6 eV for Py-DHP monolayer on ZnO(0001) and ZnO(000-1), respectively; nevertheless, the qualitative larger reduction of ϕ for ZnO(000-1) is reproduced by the calculations, thus indicating that the simulations correctly grasp the relative variations in the plane-averaged dipole moment at the interface. On one hand, the quantitative discrepancy might originate from the fact that the partial charge transfer is not quantitatively described due to the underestimation of the ZnO energy gap in the calculations; yet, it is unlikely that this effect could explain a difference of 1 eV between theory and experiment in view of the weak interfacial interactions. On the other hand, the discrepancy might originate from a wrong description of the actual spatial distribution of the charge transferred at the interface. Indeed, for small unit cells, DFT calculations are bound to create an interface dipole by transferring partial charges between the two components. We cannot thus account for a situation where a full charge is transferred to one molecule whereas the neighboring molecules remain neutral. In the following, this is shown to an important further aspect that helps understanding the experimentally observed ϕ changes.

Table 1. Theoretical decomposition of the work function shift ($\Delta\phi$) upon adsorption of the Py-DHP monolayer. All values are in the unit of eV.

	$\Delta V_{Py\text{-}DHP}$	BD	$\Delta\phi_{ZnO}$	$\Delta\phi$
On ZnO(0001)				
Closed	−1.6	0.2	0.2	−1.2
Open	−1.6	0.2	0.2	−1.2
On ZnO(000-1)				
Closed	−1.5	−0.4	0.3	−1.6
Open	−1.5	−0.3	0.2	−1.6

If we were to apply the calculated magnitude of the molecular dipole induced work function shift $\Delta V_{Py\text{-}DHP}$ (1.5–1.6 eV) to the experimental data (as schematically done in **Figure 5**), the Py-DHP LUMO would come to lie far below E_F. Electronic equilibrium would then be established by electron transfer from ZnO into Py-DHP. This, in turn, leads to a charge transfer induced interfacial dipole ΔV_{CT}, which raises the LUMO again above E_F. The fact that the ϕ values of Py-DHP monolayers on both ZnO surfaces are the same (3.7 eV), even though the pristine ZnO ϕ values are not (3.7 and 4.2 eV), further supports the notion that the electronic level alignment is governed by the ΔV_{CT}-induced shifting of the Py-DHP LUMO, a mechanism known as Fermi level pinning. We resort in the following to electrostatic considerations that have proven to explain Fermi level pinning scenarios with organic molecules very well.[29,30] The pinning-induced charge transfer most likely does not depolarize the molecular dipole, since the LUMO (where charge would be transferred to) is predominantly located on the dihydropyrene moiety of the molecule (shown in Figure S6, Supporting Information), whereas the intrinsic molecular dipole is localized within the pyridine moiety. Accordingly, we propose that in our systems the superposition of electrostatic potentials due to molecular dipoles $\Delta V_{Py\text{-}DHP}$ and pinning-induced charge transfer ΔV_{CT} determine the actual energy level positions. In such a scenario, integer electrons are transferred to a fraction of the Py-DHP molecules whereas neighboring ones remain charge-neutral, as they also feel the electrostatic potential change of their charged neighbors, which lifts their LUMO above E_F, as detailed in the following. We consider the model depicted in Figure 5c, where some Py-DHP molecules have accepted an electron due to Fermi level pinning at the LUMO (indicated by the "−" sign) and are surrounded by neutral molecules (not drawn in Figure 5c for better visibility). In this model, the change in electrostatic potential induced by the charged molecules lifts the energy levels of the neutral ones, so that they are not Fermi level pinned. In this electrostatic model, analogous to literature examples,[29] we can quantify the position of the Py-DHP frontier energy levels upon establishing electronic equilibrium as enforced by Fermi level pinning. The charged molecules are considered as a regular mesh of dipoles consisting of a positive point charge right at the ZnO surface and its negative counter charge in the molecule (see Figure 5c and further details in the Supporting Information).[31] For the location of the negative counter charge, whose spatial distribution in the molecule is *a priori* unknown, we choose a range of values along the Py-DHP backbone (Figure S7, Supporting Information), since the LUMO is mainly located there. We find that to cancel the calculated molecular dipole [fully on ZnO(0001) and in adequate part on ZnO(000-1)], that is, to reach electronic equilibrium, the fraction of charged Py-DHP molecules is 10% on both surfaces (Table S4, Supporting Information). In this case, it is understandable that charged molecules in UPS and XPS were not readily detected. As indicated above, the distribution of charged molecules results in a significant potential energy inhomogeneity right on top and

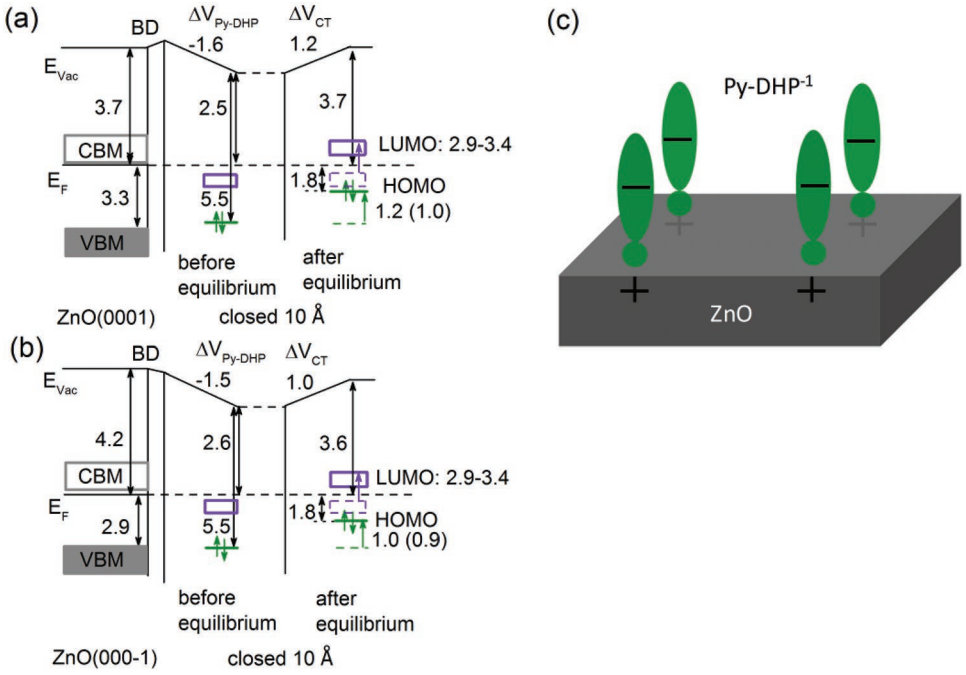

Figure 5. a,b) Fermi level pinning of closed Py-DHP on ZnO(0001) and ZnO(000-1). Before equilibrium, the frontier levels of Py-DHP are located below the Fermi level due to the potential drop created by the intramolecular dipoles. After equilibrium, HOMO levels of closed Py-DHP are located at 1.8 eV below the Fermi level. This corresponds to 1.2 and 1.0 eV upshifts of negatively charged Py-DHP ($Py\text{-}DHP^{-1}$) levels on ZnO(0001) and ZnO(000-1), respectively. The mapping of electrostatic potential in the uncharged Py-DHP region shows ≈1.0 eV (shown in the parentheses) potential increase, which agrees well with the measured HOMO onset. c) Schematic illustration of the $Py\text{-}DHP^{-1}$ molecules on ZnO, while the surrounding neutral Py-DHP is not shown.

within the Py-DHP monolayer. This can be seen from the contour plots (see Figures S8 and S9, Supporting Information) in vicinity of the monolayer (vertical distance $z = 1.4$ nm), which evidence a potential variation between charged and neutral molecular regions of ≈0.2–0.3 eV. Importantly, this energetic disorder helps rationalizing how the experimentally estimated LUMO position of the majority of (neutral) molecules in the monolayer (0.5 eV) is rather far from E_F (see Figure 5 and Figure S10, Supporting Information), while yet Fermi level pinning is established.[29]

Having identified the energy level alignment mechanisms of the monolayer and the switching process, we now turn toward the multilayer regime. For this, it is necessary to recall that the HOMO level positions of the open and closed isomers were found to be the same as for the monolayer. Yet, the work function values observed for multilayer Py-DHP on both ZnO faces are hundreds of meV higher as compared to the monolayer regime. This applies to both the open and closed isomers in the multilayer (as summarized in Figure 3), which then directly translates into higher apparent ionization energies as well. The fact that higher IE of Py-DHP persists in multilayers evidences that molecular polarization effects do not play a role. Rather, this implies a change of the (preferential) molecular orientation going from mono- to multilayer coverage,[32,33] plausibly because the pyridine group of molecules in multilayers cannot anchor anymore to the ZnO substrate. In the present case, we suggest a more lying down or at least on average a less upright orientation of Py-DHP in multilayers. To corroborate orientational changes in multilayers, we performed electronic structure calculations with PBC conditions for systems comprising a second Py-DHP layer with a lying down orientation on top of the standing Py-DHP monolayer on ZnO (shown in **Figure 6**). We first calculate the frontier levels of the isolated lying-down Py-DHP monolayer with respect to the vacuum level on the left side (shown in the upper figure) and we then place this monolayer on the ZnO/standing Py-DHP surface. This is illustrated in Figure 6, in which the energy levels are referenced to a common vacuum level at the uncovered side of the ZnO slab.[34] The negative vacuum level shift induced by the standing Py-DHP monolayer produces a downshift in the energy levels of the lying-down Py-DHP layer. In addition, this energetic alignment is preserved upon interaction of both standing and lying-down Py-DHP layers. From this, one can directly read that the IE of the lying layer is higher than the IE of the standing molecules (by 0.28 and 0.63 eV for closed and open forms). In the experiments, the higher IE of lying Py-DHP is directly reflected by the increase in work function (as mentioned earlier), since the LUMO level is in the pinning regime in the first layer (see Figure 3). To exclude any effects on the IE from the second layer being unexpectedly charged, we also performed a Bader charge analysis confirming that only negligibly charge transfer occurs into the second layer (0.07 |e| and 0.02 |e| for closed and open forms). The calculated differences in the IE of open and closed Py-DHP between the standing monolayer and the lying second layer are in good agreement with the experimentally observed values, which demonstrates that different orientations of the first and subsequent layers are a credible explanation.

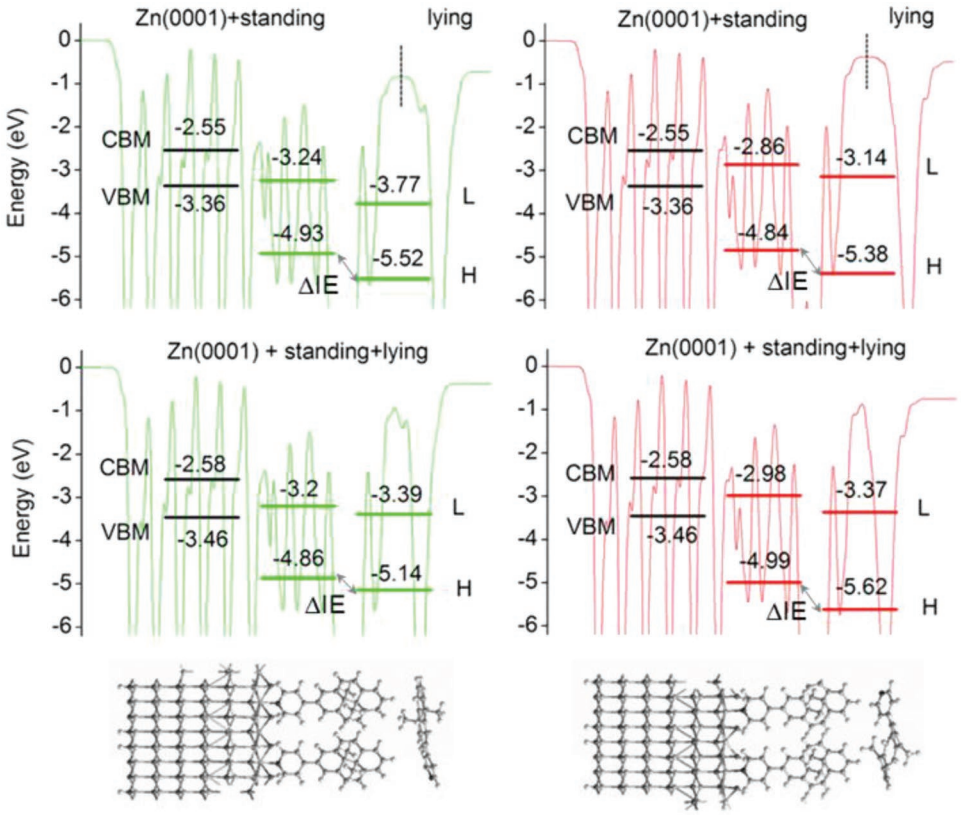

Figure 6. Energy level diagram of the multilayered Py-DHP molecules adsorbed on the ZnO(0001) surface (ZnO slab, standing and lying Py-DHP layers from left to right) for closed (green) and open (red) forms. Each graph is accompanied by the average electrostatic potential profile along the normal axis in order to help visualizing the vacuum level used as reference in the bare ZnO side. The two top graphs describe energy levels of lying Py-DHP monolayer in the isolated states with respect to ZnO/standing Py-DHP, while the two bottom graphs depict the interacting systems with lying Py-DHP monolayer brought on the surface. Note that the level alignment of noninteracting versus interacting systems is very similar, thus showing that charge transfer between standing and lying Py-DHP layers is weak. Finally, a schematic representation of the unit cell which coincides with the atomic positions in the plane average potential is represented at the bottom of the graphs.

3. Conclusions

We demonstrated experimentally that Py-DHP molecules are able to switch the electronic properties of interfaces with polar ZnO surfaces, that is, ZnO(0001) and ZnO(000-1), as further supported by DFT-based calculations. The energy level alignment at these hybrid interfaces can be reversibly modulated by external stimuli: Upon green light illumination, Py-DHP molecules switch from their closed to their open form, resulting in a substantial shift of the HOMO level by 0.7 eV (toward higher binding energy) with respect to the ZnO VBM on both polar faces. The thermal back reaction is found to be highly efficient at temperatures slightly above room temperature (50 °C). For both molecular configurations, the level alignment on both ZnO surfaces is found to be governed by Fermi level pinning at the LUMO of Py-DHP. In multilayers, we observe a work function increase by 0.3 and 0.5 eV upon photoswitching on ZnO(0001) and ZnO(000-1), respectively, leading to different ionization energies of Py-DHP compared to the monolayer. This is attributed to a change of the molecular orientation from preferentially standing up to lying down. Our findings provide a pathway for manipulating the interface electronic properties with photoswitches in a dynamic manner using light and thermal energy, and can thus be used to remote-control the electronic properties of interfaces within photoswitchable (opto-) electronic devices.

4. Experimental Section

Experimental Methods: Synthesis of Py-DHP is described in the Supporting Information. Photoemission experiments were performed in a custom-made multichamber ultrahigh vacuum (UHV) system, which consists of a fast entry load lock, a sample preparation chamber ($<5 \times 10^{-9}$ mbar), and an analysis chamber ($<2 \times 10^{-10}$ mbar). Photoelectrons were excited with He I ($h\nu = 21.22$ eV) radiation at very low excitation density, achieved by thin Al foils; under these conditions, radiation damage and charging of the sample are absent or at least minimized to an extent that they do not compromise data interpretation (for details see ref. [11]). Photoelectrons were collected and analyzed with a hemispherical spectrometer (SPECS Phoibos 100); the total instrumental energy resolution in UPS was 150 meV, as determined by measuring the Fermi edge of single-crystal Au. The secondary electron cutoff (SECO) spectra were recorded with samples biased at −10 V to clear the analyzer work function. XPS measurements were conducted using Al Kα radiation (1486.6 eV). The Fermi level is referred to as the zero-binding energy in all UPS and XPS spectra. UV–vis spectroscopy measurements were performed in a PerkinElmer Lambda 950 spectrometer.

ZnO crystals (purchased from Crystec) were cleaned in UHV by repeated cycles of Ar-ion sputtering (1 kV, 3 μA) and annealing to 400 °C. The surface cleanliness of ZnO was verified by the absence of notable carbon core level intensity in XPS. Py-DHP molecules (originally in closed form) were evaporated onto the clean ZnO surfaces from a resistively heated quartz crucible. The evaporation rate was set to 1–2 Å min^{-1} by a quartz crystal microbalance. During sample preparation, transfer, and measurements, the samples were kept in dark (or exposed to a minimum amount of light to avoid unintended switching) and without breaking vacuum. For switching, the sample was in situ either illuminated with green light (λ_{max} = 565 nm, maximum intensity is 200 mW cm^{-2}) to switch the molecule from closed to open form, or heated at a temperature of 50 °C for switching back to the closed form. Except for the sample heating for initiation of the back reaction, all measurements were performed at room temperature.

Computational Methods: Theoretical calculations were performed at the DFT level. The optimized geometry and ground-state electronic properties (frontier orbitals and dipole moment) of the isolated Py-DHP molecule were obtained using the Perdew–Burke–Ernzerhof (PBE)[35] functional and a 6-31G(d) basis set.[36] The choice of PBE is motivated by a sake of coherence with the calculations performed with periodic boundary conditions (PBC). The simulated DOS were obtained by convoluting delta functions at the molecular orbital (MO) energies with a Gaussian function having a full width at half maximum (FWHM) of 0.5 eV for an optimal comparison with the UPS spectra. TD-DFT calculations were performed to simulate the absorption spectra and assess the nature of relevant electronic excited states using the same basis set and the hybrid PBE0 functional to ensure a good comparison with experimental data.[37] The electronic properties of Py-DHP molecules on ZnO were described using the SIESTA 4.0 (Spanish Initiative for Electronic Simulations with Thousands of Atoms) computational code with PBC.[38] The valence electrons are described within the linear combination of atomic orbitals (LCAO) approximation, with a double zeta polarized (DZP) basis set; the valence-core interactions are described by Troulier-Martins pseudopotentials.[39] Following a previous work,[27] DFT calculations were performed within the generalized gradient approximation (GGA) by using the PBE exchange correlation functional.[35] The mesh cutoff used is 190 Ry. According to the surface density (2.6 ± 0.8 molecules nm^{-2}, see the Supporting Information) of Py-DHP monolayer on ZnO as estimated from XPS, the unit cells of polar ZnO faces (for standing Py-DHP) were made of 12 layers with *a* and *b* lattice vectors of 6.5 and 5.6 Å, respectively. This yields a theoretical surface density of ≈2.8 molecules nm^{-2}, comparable to the experimental data. For lying Py-DHP molecules, in the absence of experimental coverage, a larger unit cell with a = 13 Å and b = 11.2 Å was used, respectively. The surface density of lying Py-DHP is 0.7 molecules nm^{-2} (see the Supporting Information for the detailed structure). The surface and bottom part of ZnO slabs are homogeneously covered with OH groups and H atoms at 50% of coverage to prevent the "metallization effect."[40] The calculated bandgaps are ≈1 eV for both polar ZnO faces, which are smaller than the experimentally measured results (3.3 eV),[41] though without major implications for the calculated work function shifts. For all calculations, a (3 × 3 × 1) Monkhorst–Pack k-point grid[42] was used to describe the electronic structure in the first Brillouin zone. In order to fasten the geometry optimizations, the bottom six layers were frozen and only the top six layers were relaxed.

Supporting Information

Supporting Information is available from the Wiley Online Library or from the author.

Acknowledgements

This work was financially supported by the EC through the Marie Curie project ITN iSwitch (Grant Agreement No. 642196) and the Deutsche Forschungsgemeinschaft (DFG) – Projektnummer 182087777 – SFB 951. Computational resources were provided by the Consortium des Équipements de Calcul Intensif (CÉCI) funded by the Belgian National Fund for Scientific Research (F.R.S.-FNRS) under Grant No. 2.5020.11. J.C. is an FNRS research director.

Conflict of Interest

The authors declare no conflict of interest.

Keywords

density functional theory, dihydropyrene, photochromism, photoemission spectroscopy, ZnO

Received: January 31, 2019
Revised: March 10, 2019
Published online:

[1] N. Bano, S. Zaman, A. Zainelabdin, S. Hussain, I. Hussain, O. Nur, M. Willander, *J. Appl. Phys.* **2010**, *108*, 043103.
[2] K. Nomura, H. Ohta, A. Takagi, T. Kamiya, M. Hirano, H. Hosono, *Nature* **2004**, *432*, 488.
[3] D. C. Olson, J. Piris, R. T. Collins, S. E. Shaheen, D. S. Ginley, *Thin Solid Films* **2006**, *496*, 26.
[4] H. G. Li, G. Wu, M. M. Shi, L. G. Yang, H. Z. Chen, M. Wang, *Appl. Phys. Lett.* **2008**, *93*, 153309.
[5] Y. Y. Lin, Y. Y. Lee, L. Chang, J. J. Wu, C. W. Chen, *Appl. Phys. Lett.* **2009**, *94*, 2007.
[6] R. Schlesinger, F. Bianchi, S. Blumstengel, C. Christodoulou, R. Ovsyannikov, B. Kobin, K. Moudgil, S. Barlow, S. Hecht, S. R. Marder, F. Henneberger, N. Koch, *Nat. Commun.* **2015**, *6*, 6754.
[7] F. Piersimoni, R. Schlesinger, J. Benduhn, D. Spoltore, S. Reiter, I. Lange, N. Koch, K. Vandewal, D. Neher, *J. Phys. Chem. Lett.* **2015**, *6*, 500.
[8] M. T. Greiner, M. G. Helander, W. M. Tang, Z. B. Wang, J. Qiu, Z. H. Lu, *Nat. Mater.* **2012**, *11*, 76.
[9] R. Schlesinger, Y. Xu, O. T. Hofmann, S. Winkler, J. Frisch, J. Niederhausen, A. Vollmer, S. Blumstengel, F. Henneberger, P. Rinke, M. Scheffler, N. Koch, *Phys. Rev. B* **2013**, *87*, 155311.
[10] S. Braun, W. R. Salaneck, M. Fahlman, *Adv. Mater.* **2009**, *21*, 1450.
[11] Q. Wang, J. Frisch, M. Herder, S. Hecht, N. Koch, *ChemPhysChem* **2017**, *18*, 722.
[12] E. Orgiu, P. Samorì, *Adv. Mater.* **2014**, *26*, 1827.
[13] T. Mosciatti, M. G. del Rosso, M. Herder, J. Frisch, N. Koch, S. Hecht, E. Orgiu, P. Samorì, *Adv. Mater.* **2016**, *28*, 6606.
[14] R. Klajn, *Chem. Soc. Rev.* **2014**, *43*, 148.
[15] M. Irie, T. Fukaminato, K. Matsuda, S. Kobatake, *Chem. Rev.* **2014**, *114*, 12174.
[16] E. Orgiu, N. Crivillers, M. Herder, L. Grubert, M. Pätzel, J. Frisch, E. Pavlica, D. T. Duong, G. Bratina, A. Salleo, N. Koch, S. Hecht, P. Samorì, *Nat. Chem.* **2012**, *4*, 675.
[17] D. Roldan, V. Kaliginedi, S. Cobo, V. Kolivoska, C. Bucher, W. Hong, G. Royal, T. Wandlowski, *J. Am. Chem. Soc.* **2013**, *135*, 5974.
[18] M. M. Russew, S. Hecht, *Adv. Mater.* **2010**, *22*, 3348.
[19] Y. Garmshausen, K. Klaue, S. Hecht, *ChemPlusChem* **2017**, *82*, 1025.
[20] D. Roldan, S. Cobo, F. Lafolet, N. Vilà, C. Bochot, C. Bucher, E. Saint-Aman, M. Boggio-Pasqua, M. Garavelli, G. Royal, *Chem. - Eur. J.* **2015**, *21*, 455.

[21] A. Bakkar, S. Cobo, F. Lafolet, E. Saint-Aman, G. Royal, *J. Mater. Chem. C* **2015**, *3*, 12014.
[22] A. Bakkar, F. Lafolet, M. Boggio-Pasqua, D. Jouvenot, E. Saint-Aman, S. Cobo, *Chem. Commun.* **2017**, *53*, 9360.
[23] O. T. Hofmann, J. C. Deinert, Y. Xu, P. Rinke, J. Stähler, M. Wolf, M. Scheffler, *J. Chem. Phys.* **2013**, *139*, 174701.
[24] P. K. Nayak, N. Periasamy, *Org. Electron.* **2009**, *10*, 1396.
[25] W. Gao, A. Kahn, *Appl. Phys. Lett.* **2003**, *82*, 4815.
[26] L. Chen, R. Ludeke, X. Cui, A. G. Schrott, C. R. Kagan, L. E. Brus, *J. Phys. Chem. B* **2005**, *109*, 1834.
[27] D. Cornil, T. Van Regemorter, D. Beljonne, J. Cornil, *Phys. Chem. Chem. Phys.* **2014**, *16*, 20887.
[28] C. Wood, H. Li, P. Winget, J. L. Bredas, *J. Phys. Chem. C* **2012**, *116*, 19125.
[29] P. Amsalem, J. Niederhausen, A. Wilke, G. Heimel, R. Schlesinger, S. Winkler, A. Vollmer, J. P. Rabe, N. Koch, *Phys. Rev. B* **2013**, *87*, 35440.
[30] J. Niederhausen, P. Amsalem, A. Wilke, R. Schlesinger, S. Winkler, A. Vollmer, J. P. Rabe, N. Koch, *Phys. Rev. B* **2012**, *86*, 81411.
[31] B. J. Topham, M. Kumar, Z. G. Soos, *Adv. Funct. Mater.* **2011**, *21*, 1931.
[32] G. Heimel, I. Salzmann, S. Duhm, N. Koch, *Chem. Mater.* **2011**, *23*, 359.
[33] S. Duhm, G. Heimel, I. Salzmann, H. Glowatzki, R. L. Johnson, A. Vollmer, J. P. Rabe, N. Koch, *Nat. Mater.* **2008**, *7*, 326.
[34] G. Heimel, L. Romaner, J.-L. Brédas, E. Zojer, *Phys. Rev. Lett.* **2006**, *96*, 196806.
[35] J. P. Perdew, K. Burke, M. Ernzerhof, *Phys. Rev. Lett.* **1996**, *77*, 3865.
[36] V. A. Rassolov, M. A. Ratner, J. A. Pople, P. C. Redfern, L. A. Curtiss, *J. Comput. Chem.* **2001**, *22*, 976.
[37] C. Adamo, V. Barone, *J. Chem. Phys.* **1999**, *110*, 6158.
[38] J. M. Soler, E. Artacho, J. D. Gale, A. Garcia, J. Junquera, P. Ordejon, D. Sanchez-Portal, *J. Phys.: Condens. Matter* **2002**, *14*, 2745.
[39] N. Troullier, J. L. Martins, *Phys. Rev. B* **1991**, *43*, 8861.
[40] H. Li, L. K. Schirra, J. Shim, H. Cheun, B. Kippelen, O. L. A. Monti, J. L. Bredas, *Chem. Mater.* **2012**, *24*, 3044.
[41] V. Srikant, D. R. Clarke, *J. Appl. Phys.* **1998**, *83*, 5447.
[42] J. D. Pack, H. J. Monkhorst, *Phys. Rev. B* **1977**, *16*, 1748.

